LVQ-VAE:END-TO-END HYPERPRIOR-BASED VARIATIONAL IMAGE COMPRESSION WITH LATTICE VECTOR QUANTIZATION

Anonymous authors
Paper under double-blind review

ABSTRACT

Image compression technology has become more important research topic. In recent years, learning-based methods have been extensively studied and variational autoencoder (VAE)-based methods using hyperprior-based context-adaptive entropy model have been reported to be comparable to the latest video coding standard H.266/VVC in terms of RD performance. We think there is room for improvement in quantization process of latent features by adopting vector quantization (VQ). Many VAE-based methods use scalar quantization for latent features and do not exploit correlation between the features. Although there are methods that incorporate VQ into learning-based methods, to the best our knowledge, there are no studies that utilizes the hyperprior-based VAE with VQ because incorporating VQ into a hyperprior-based VAE makes it difficult to estimate the likelihood. In this paper, we propose a new VAE-based image compression method using VQ based latent representation for hyperprior-based context-adaptive entropy model to improve the coding efficiency. The proposed method resolves problem faced by conventional VQ-based methods due to codebook size bloat by adopting Lattice VQ as the basis quantization method and achieves end-to-end optimization with hyperprior-based context-adaptive entropy model by approximating the likelihood calculation of latent feature vectors with high accuracy using Monte Carlo integration. Furthermore, in likelihood estimation, we model each latent feature vector with multivariate normal distribution including covariance matrix parameters, which improves the likelihood estimation accuracy and RD performance. Experimental results show that the proposed method achieves a state-of-the-art RD performance exceeding existing learning-based methods and the latest video coding standard H.266/VVC by 18.0 % for Kodak, 21.9 % for CLIC2022 and 39.2 % for Tecnick.

1 INTRODUCTION

Image compression technology has become more important than ever to achieve efficient data transmission and storage due to the demand for of high-quality contents and the increase in the popularity of video services. Various conventional image compression technologies have been standardized so far (JPEG (Wallace, 1991; ITU, 1993), JPEG2000 (Taubman & Marcellin, 2002; ISO/TEC, 2004), WebP (Google), H.264/AVC (Marpe et al., 2006; ISO/IEC, 2003), H.265/HEVC (Sullivan et al., 2012; ISO/IEC, 2013), H.266/VVC (Bross et al., 2021; ISO/IEC, 2020), etc.). These technologies consist of a combination of transform, quantization and entropy coding. Transform is a major part of JPEG, H.265/HEVC and H.266/VVC which use DCT or DST, while JPEG2000 uses wavelet transform, all of which are based on handcrafted linear transforms. These hand-crafted design are limited in their ability to capture features for a variety of images.

In recent years, deep learning has made remarkable progress, and learning-based methods are being actively explored in the field of image compression. Most recent learning-based methods are based on transform coding (Goyal, 2001). Many of these methods use convolutional neural network (CNN)-based autoencoders in which the encoder transforms the input image into a latent representation and then performs quantization and entropy coding, while the decoder reconstructs the restored image. This approach achieves flexible nonlinear transforms that have higher potential to

map pixels into a more compressible latent representation than the linear transforms used by classical image compression approaches. It can be divided into two types according to the metric used for encoder optimization. One is the generative approach that directly maximizes subjective image quality (Rippel & Bourdev, 2017; Santurkar et al., 2018; Agustsson et al., 2019; Mentzer et al., 2020; Kudo et al., 2021). This approach aims to optimize the distribution of reconstructed images to approach that of natural images by using generative adversarial networks. The other maximizes an objective metric such as peak signal-to-noise ratio (PSNR). This approach solves the rate-distortion (RD) optimization problem in the same way as the classical image compression described above. This paper focuses on the latter approach as it is applicable to a wider range of applications. The latter approach is found in various proposals. Toderici et al. (2016; 2017) introduced recurrent neural networks for feature extraction and Johnston et al. (2017) enhanced these networks to improve the coding performance. Cai & Zhang (2018); Cai et al. (2018) directly trained the quantization. These methods quantize the latent features as fixed-length codes.

By contrast, variational autoencoder (VAE)-based methods have been proposed that formulate the optimization as the problem of minimizing the entropy of the quantized latent features as well as the expected distortion of the reconstructed image with respect to the original. The first image compression method using VAE was proposed by Theis et al. (2017) and Ballé et al. (2017). They studied entropy models to approximate the actual distributions of the quantized latent features. To improve the accuracy of the entropy model, a hyperprior-based context-adaptive entropy model was proposed by Ballé et al. (2018); it has been the baseline in most subsequent research. Whereas the actual distributions of each latent feature are fixed in (Theis et al., 2017; Ballé et al., 2017), Ballé et al. (2018) approximated the entropy model as a zero-mean Gaussian distribution with scale parameter for each latent feature to remove the spatial redundancy, where contexts are encoded as side information. Based on this hyperprior-based context-adaptive entropy model, various methods have been proposed to estimate the entropy model with higher accuracy. The autoregressive context model is one of the technologies that has experienced significant performance improvements. Minnen et al. (2018) and Lee et al. (2019) proposed to jointly utilize an autoregressive context model and the mean and scale hyperpriors. Mentzer et al. (2018) and Chen et al. (2021) extended an autoregressive context model that utilizes channel neighbors with 3D Masked Convolution module. In (Minnen & Singh, 2020) and (Zhu et al., 2022b), the channel-directed autoregressive model was applied to reduce the computational complexity of the spatial-directed autoregressive model and He et al. (2022) was further improved by dividing the model non-evenly into channel directions. To further improve the entropy model, Liu et al. (2020) and Cheng et al. (2020) proposed a Gaussian mixture model and developed a network architecture by adopting an attention module. As another improvement perspective, Hu et al. (2020) proposed coarse-to-fine hyperprior modeling while Yang et al. (2020) improved the performance by devising an inference process without changing the training process. Ho et al. (2021) and Xie et al. (2021) focused on improving the network architecture by adopting a normalizing flow module. Some methods have been reported to better the RD performance of H.266/VVC, the latest video coding standard, which is not learning based, in terms of the MS-SSIM metric, but are still comparable in the PSNR metric.

Vector quantization (VQ) is incorporated into learning-based methods to leverage performance. Since VQ potentially offers better performance than scalar quantization in terms of RD (Gray & Neuhoff, 1998; Gray, 1984; Chou et al., 1989), various studies have examined it (Shin & Lu, 1991; Antonini et al., 1992; Tatsaki et al., 1995; Shnaider & Paplinski, 2001; Voinson et al., 2002; Salleh & Soraghan, 2007; Chiranjeevi & Jena, 2018; Nag, 2019). The challenge in applying VQ to learning-based compression methods is how to incorporate the likelihood estimation of latent feature vectors into the optimization process. van den Oord et al. (2017) proposed VQ-VAE which avoids likelihood calculations by assuming uniformity of the prior distribution of latent features and separately designing encoder/decoder and codebooks to perform gradient optimization. Razavi et al. (2019) and Fauw et al. (2019) extended VQ-VAE to a hierarchical network structure. Williams et al. (2020) revised the quantization process while Xue et al. (2019) combined optimization with supervised learning. However, all of the above methods do not perform well because the learning parameters underlying the encoder/decoder and codebook are designed separately to achieve gradient optimization and/or the probability distribution is assumed to be uniform. Agustsson et al. (2017) attempts end-to-end optimization by performing VQ using a soft-to-hard annealing strategy. However, its learning suffers from unstable convergence, because it approximates the prior distribution of the codebook with a histogram taken from the training process. Zhu et al. (2022a) proposed a cascaded vector quantization with multi-codebooks to keep memory

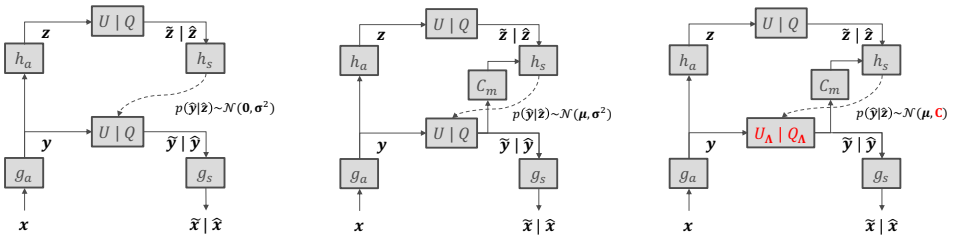

(a) Baseline (b) Autoregressive (c) Proposed (key features are noted by red)

Figure 1: Operational diagrams of VAE-based image compression. $U \mid Q$ and $U_{\mathbf{\Lambda}} \mid Q_{\mathbf{\Lambda}}$ represents either quantization during training (producing variables with a tilde) or quantization during inference (producing variables with a hat).

capacity and performance at high bitrates. However, due to the limitation on the vector dimension, this approach does not fully utilize the potential performance of vector quantization. In addition, to the best knowledge of the authors, no study has utilized the above-mentioned hyperprior-based context-adaptive entropy model with VQ. Incorporating VQ into the hyperprior-based method and optimizing them in an end-to-end manner has not been achieved, because incorporating VQ into a hyperprior-based context-adaptive entropy model makes it difficult to estimate the likelihood.

In this paper, we propose a new VAE-based image compression method using VQ-based latent representation for a hyperprior-based context-adaptive entropy model (named LVQ-VAE) with improved coding efficiency. The proposed method has two main features. First we introduce Lattice VQ for quantization, which resolves the codebook size bloat problem faced by conventional VQ-based methods without coding efficiency degradation. At the same time, the proposed method achieves end-to-end optimization with the hyperprior-based context-adaptive entropy model by using Monte Carlo integration to approximate with high accuracy the likelihood calculation of latent feature vectors. Second, in likelihood estimation, we model each latent feature vector as a multivariate normal distribution including covariance matrix parameters, which improves the likelihood estimation accuracy and RD performance. Zhu et al. (2022a) also models latent feature vectors as a multivariate normal distribution, but this method models the features contained in each representative point as a single distribution, whereas the proposed method models each feature vector, which eliminates correlation among feature vectors and is expected to improve coding performance.

The contributions of this paper are summarized as follows:

- We incorporate VQ into VAE-based image compression method using hyperprior-based context-adaptive entropy model while optimizing them for end-to-end manner, which leads to obtain better RD performance that exceeds the limits possible with scalar quantization without codebook size bloat.
- We improve the entropy model by modeling each latent feature vector as a multivariate normal distribution including covariance matrix parameters, which improves RD performance.
- We show that the proposed method achieves state-of-the-art RD performance compared to existing learning-based methods and the latest video coding standard H.266/VVC with regard to the PSNR metric.

2 VAE-BASED IMAGE COMPRESSION

Most recent VAE-based methods are based on the hyperprior model developed by Ballé et al. (2018) as shown in Fig. 1 (a). This model consists of four parametric transforms:

- $g_a(\boldsymbol{x}; \boldsymbol{\phi}_g)$: a feature encoder that transforms input image $\boldsymbol{x}$ into latent feature $\boldsymbol{y}$, which is quantized to form $\hat{\boldsymbol{y}} = Q(\boldsymbol{y})$,
- $g_s(\hat{\boldsymbol{y}}; \boldsymbol{\theta}_g)$: a feature decoder that reconstructs image $\hat{\boldsymbol{x}} = g_s(\hat{\boldsymbol{y}}; \boldsymbol{\theta}_g)$,

- $h_a(\boldsymbol{y}; \boldsymbol{\phi}_h)$: a hyper-encoder that extracts latent representation $\boldsymbol{z}$ for context information, which is quantized to form $\hat{\boldsymbol{z}} = Q(\boldsymbol{z})$,
- $h_s(\hat{\boldsymbol{z}}; \boldsymbol{\theta}_h)$: a hyper-decoder that generates the context information for estimating the entropy model $p_{\hat{\boldsymbol{y}}|\hat{\boldsymbol{z}}}(\hat{\boldsymbol{y}} \mid \hat{\boldsymbol{z}})$.

$\boldsymbol{\phi}_g, \boldsymbol{\theta}_g, \boldsymbol{\phi}_h, \boldsymbol{\theta}_h$ are optimized parameters of each transform, which are generally composed of neural networks such as CNNs. $U \,|\, Q$ denotes a quantizer in a training phase (U) and one in an inference phase (Q). In the training phase, quantizer U is approximated using additive uniform noise as $\tilde{\boldsymbol{y}} = U(\boldsymbol{y}) = [y_1 + u_1, \ldots, y_N + u_N]$, where u_i is sampled from univariate uniform distribution $\mathcal{U}(-\frac{1}{2}, \frac{1}{2})$. This is because end-to-end learning requires the quantization to realize gradient-based optimization. In addition to the above approximation, several other approximation techniques have been studied, such as stochastic binarization (Toderici et al., 2016), universal quantization (Choi et al., 2019), straight-through estimator (van den Oord et al., 2017), and soft-to-hard quantization (Agustsson et al., 2017). In the inference phase, quantizer Q is actual quantization such as a rounding operator. In this manuscript, we represent approximated data as a variable with a tilde and quantized data as one with a hat as shown in Fig. 1.

The encoder compresses latent representation $\hat{\boldsymbol{y}}$ and $\hat{\boldsymbol{z}}$ by using entropy coding such as arithmetic coding (Rissanen & Langdon, 1979) and transmits it as a bitstream. The entropy coding estimates probability $p_{\hat{\boldsymbol{y}}|\hat{\boldsymbol{z}}}(\hat{\boldsymbol{y}} \mid \hat{\boldsymbol{z}})$ as zero-mean Gaussian $\mathcal{N}(\mathbf{0}, \boldsymbol{\sigma}^2)$; its context information is scale parameter $\boldsymbol{\sigma} = h_s(\hat{\boldsymbol{z}}; \boldsymbol{\theta}_h)$. To further improve this estimation, Minnen et al. (2018) and Lee et al. (2019) jointly utilized the autoregressive model and the mean and scale parameters of Gaussian distribution (Fig. 1 (b)), where C_m denotes a context prediction model conditioned on decoded features that are composed of an autoregressive module such as masked convolutions (van den Oord et al., 2016). As for $p_{\hat{\boldsymbol{z}}}(\hat{\boldsymbol{z}})$, the non-adaptive fixed density model called factorized prior is trained and shared between the encoder and the decoder.

Finally, the learning process is formulated as RD optimization which minimizes the following loss function.

$$\begin{aligned} \mathcal{L} &= \mathcal{R} + \lambda \cdot \mathcal{D} \\ &= \mathbb{E}_{\boldsymbol{x} \sim p_{\boldsymbol{x}}} \left[-\log p_{\tilde{\boldsymbol{y}}|\tilde{\boldsymbol{z}}}(\tilde{\boldsymbol{y}} \mid \tilde{\boldsymbol{z}}) - \log p_{\tilde{\boldsymbol{z}}}(\tilde{\boldsymbol{z}}) \right] + \lambda \cdot \mathbb{E}_{\boldsymbol{x} \sim p_{\boldsymbol{x}}} \left\| \boldsymbol{x} - \tilde{\boldsymbol{x}} \right\|_2^2 \end{aligned} \tag{1}$$

where $p_{\boldsymbol{x}}$ is the marginal distribution of natural images, and $\mathcal{D}$ represents the expected distortion between the reconstructed image and the original, and $\mathcal{R}$ represents the entropy of $\tilde{\boldsymbol{y}}$ and $\tilde{\boldsymbol{z}}$ that approximates the expected code length of the bitstream. λ is the Lagrange multiplier that controls the RD trade-off.

3 Proposed Method

The proposed method has two key features:

1. We introduce Lattice VQ for quantization of the latent features $\boldsymbol{y}$, as this achieves better RD performance than scalar quantization without codebook size bloat.
2. We model each latent feature vector with a multivariate normal distribution including covariance matrix parameters and incorporate it into the autoregressive model to achieve highly accurate likelihood estimation.

Figure 1 (c) shows the operational diagram of the proposed method. In the following, we will describe a quantizer design based on Lattice VQ and then explain how to incorporate it into a hyperprior-based context-adaptive entropy model.

3.1 Quantizer design based on Lattice Vector Quantization

We use Lattice VQ for quantizing latent feature $\boldsymbol{y}$. Given N elements of features denoted by $y_1, \ldots, y_N$, the features are split into n-dimensional vectors $\boldsymbol{v}_1, \ldots, \boldsymbol{v}_{\lceil N/n \rceil}$ as follows.

$$\boldsymbol{v}_i = \left[y_{ni-n+1}, y_{ni-n+2}, \ldots, y_{ni} \right], 1 \leq i \leq \lceil N/n \rceil \tag{2}$$

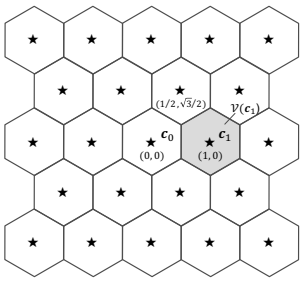

Figure 2: A_2 lattice

Then these n-dimensional vectors are divided into clusters, and each cluster is represented by its centroid point.

Lattice VQ is a VQ that places representative points at the location to form a lattice. Lattice $\mathbf{\Lambda} \in \mathbb{R}^n$ is formed as a linear combination of basis vectors (Conway & Sloane, 1988):

$$\mathbf{\Lambda} = \left\{ \sum_i^n k_i \boldsymbol{b}_i \mid k_i \in \mathbb{Z} \right\} \tag{3}$$

where $\boldsymbol{b}_1, \ldots, \boldsymbol{b}_n$ are basis vectors for $\mathbb{R}^n$, and a matrix with these basis vectors as column vectors is also called the generating matrix which is uniquely defined for the structure of lattice, and k_i is an integer coefficient. For example, the 2-dimensional hexagonal lattice A_2 is shown in Fig. 2. The lattice points $\boldsymbol{c} \in \mathbf{\Lambda}$ are the representative points of Lattice VQ. Let $Q_{\mathbf{\Lambda}}(\boldsymbol{v})$ be the nearest neighbor of $\boldsymbol{v}$ in terms of Euclidean norm in the lattice:

$$Q_{\mathbf{\Lambda}}(\boldsymbol{v}) = \{\boldsymbol{c}_i : \|\boldsymbol{v} - \boldsymbol{c}_i\| \leq \|\boldsymbol{v} - \boldsymbol{c}_j\|, \boldsymbol{c}_i, \boldsymbol{c}_j \in \mathbf{\Lambda} \text{ for all } j \neq i\} \tag{4}$$

The Voronoi region of lattice point $\boldsymbol{c}_i$ is the set of all vectors mapped into this point as defined by

$$\mathcal{V}(\boldsymbol{c}_i) = \{\boldsymbol{v} : \|\boldsymbol{v} - \boldsymbol{c}_i\| \leq \|\boldsymbol{v} - \boldsymbol{c}_j\|, \boldsymbol{c}_i, \boldsymbol{c}_j \in \mathbf{\Lambda} \text{ for all } j \neq i\} \tag{5}$$

Key features of Lattice VQ are follows:

1. A fast quantization method has been developed. Several lattices (A_2, D_4 (4-dimensional checkerboard root lattice), E_8 (8-dimensional Gosset's root lattice), Λ_{24} (24-dimensional Leech lattice), etc.) have fast quantization methods (Conway & Sloane, 1982; 1986; Vardy & Be'ery, 1993), and there are also fast iterative methods such as (Agrell et al., 2002) for arbitrary lattices.
2. Lattice VQ with a particular generator matrix such as A_2, D_4, E_8, Λ_{24} is an optimal quantizer minimizing the distortion for uniform distribution source.

In terms of effectively utilizing the potential of Lattice VQ, we set the vectorization axis in the channel direction. There are two reasons for this. One is that the autoregressive model based on a pixel-by-pixel update cannot be applied when the vectorization axis is set in the spatial direction. The other is that most conventional VAE-based methods do not take account of correlations in the channel direction. Although Minnen & Singh (2020); Zhu et al. (2022b); He et al. (2022) apply autoregressive models in the channel direction, the distribution of latent features is indirectly predicted using features obtained by AR models. By contrast, the proposed method predicts the distribution of latent features directly, which is expected to improve performance.

To perform end-to-end optimization with the gradient method, we employ the approximation method proposed by Lee et al. (2019), that is, we use straight-through estimator (STE) (Courbariaux & Bengio, 2016) for a decoder and the additive noise (Ballé et al., 2018) for the entropy model. Unlike when using additive noise for both as is common in most conventional methods, this method can eliminate train-test mismatch. Let $\mathcal{U}_{\mathcal{V}_\mathbf{0}}$ be a n-dimensional random variable uniformly distributed over the basic cell of the lattice $\mathcal{V}_\mathbf{0} = \mathcal{V}(\mathbf{0})$, the Voronoi region of the lattice

point $\mathbf{0}$. We generate $\boldsymbol{u}_i \sim \mathcal{U}_{\mathcal{V}_\mathbf{0}}$ and perform the following process.

$$\tilde{\boldsymbol{v}}_i = U_{\boldsymbol{\Lambda}}(\boldsymbol{v}_i) = \begin{cases} Q^{\text{STE}}_{\boldsymbol{\Lambda}}(\boldsymbol{v}_i) & \text{for a decoder} \\ \boldsymbol{v}_i + \boldsymbol{u}_i & \text{for an entropy model} \end{cases} \quad \text{(in training)} \tag{6}$$

$$\hat{\boldsymbol{v}}_i = Q_{\boldsymbol{\Lambda}}(\boldsymbol{v}_i) \quad \text{(in inference)} \tag{7}$$

where $Q^{\text{STE}}_{\boldsymbol{\Lambda}}$ is the same as $Q_{\boldsymbol{\Lambda}}$ but its gradient is $\frac{\partial}{\partial \boldsymbol{v}_i}\tilde{\boldsymbol{v}}_i = \mathbf{1}$.

3.2 Probability Model

The probability entropy model for $\hat{\boldsymbol{v}}$ is represented as

$$p_{\hat{\boldsymbol{v}}|\hat{\boldsymbol{z}}}(\hat{\boldsymbol{v}} \mid \hat{\boldsymbol{z}}) = \prod_{i=1}^{\lceil N/n \rceil} p_{\hat{\boldsymbol{v}}_i|\hat{\boldsymbol{z}}}(\hat{\boldsymbol{v}}_i \mid \hat{\boldsymbol{v}}_{<i}, \hat{\boldsymbol{z}}) \tag{8}$$

where $\hat{\boldsymbol{v}}_{<i} = [\hat{\boldsymbol{v}}_1, \hat{\boldsymbol{v}}_2, \ldots, \hat{\boldsymbol{v}}_{i-1}]$. Each element of vectorized features $\hat{\boldsymbol{v}}_i$ is modeled as a multivariate Gaussian with its own mean $\boldsymbol{\mu}_i$ and covariance matrix $\mathbf{C}_i$, where the mean and covariance matrix are jointly predicted by the hyper-decoder $h_s(\hat{\boldsymbol{z}}; \boldsymbol{\theta}_h)$ and autoregressive neural networks f_ψ consisting of masked convolution:

$$p_{\hat{\boldsymbol{v}}_i|\hat{\boldsymbol{z}}}(\hat{\boldsymbol{v}}_i \mid \hat{\boldsymbol{v}}_{<i}, \hat{\boldsymbol{z}}) = \int_{\hat{\boldsymbol{v}}_i + \mathcal{V}_\mathbf{0}} \mathcal{N}(\boldsymbol{\mu}_i, \mathbf{C}_i)(\boldsymbol{x})\, d\boldsymbol{x} \tag{9}$$

where $\boldsymbol{\mu}_i, \mathbf{C}_i$ are estimated using $f_\psi(\hat{\boldsymbol{v}}_{<i}, h_s(\hat{\boldsymbol{z}}; \boldsymbol{\theta}_h))$. As for the probability entropy model of $\hat{\boldsymbol{z}}$, we use the factorized density model that is the same method as used in the previous work (Ballé et al., 2018).

3.2.1 Covariance Matrix Estimation

It is necessary to estimate covariance matrix $\mathbf{C}_i$ to satisfy the condition of a positive definite symmetric matrix. It is known that the positive definite symmetric matrix can be generated by matrix operation on an arbitrary matrix and its transpose. Here, network $f_\psi(\hat{\boldsymbol{v}}_{<i}, h_s(\hat{\boldsymbol{z}}; \boldsymbol{\theta}_h))$ outputs mean vector $\boldsymbol{\mu}_i \in \mathbb{R}^n$ and matrix $\mathbf{A}_i \in \mathbb{R}^{n \times n}$ for each vectorized feature:

$$f_\psi(\hat{\boldsymbol{v}}_{<i}, h_s(\hat{\boldsymbol{z}}; \boldsymbol{\theta}_h)) = \begin{bmatrix} \boldsymbol{\mu}_i \\ \mathbf{A}_i \end{bmatrix} \tag{10}$$

$$\boldsymbol{\mu}_i = [\mu_1, \quad \mu_2, \quad \cdots, \quad \mu_n] \tag{11}$$

$$\mathbf{A}_i = \begin{bmatrix} a_{1,1}, & a_{1,2}, & \cdots, & a_{1,n} \\ a_{2,1}, & a_{2,2}, & \cdots, & a_{2,n} \\ \vdots & \vdots & \ddots & \vdots \\ a_{n,1}, & a_{n,2}, & \cdots, & a_{n,n} \end{bmatrix} \tag{12}$$

Then, covariance matrix $\mathbf{C}_i$ is calculated as

$$\mathbf{C}_i = \frac{1}{n}\mathbf{A}_i^T \mathbf{A}_i + \varepsilon \mathbf{I}, \tag{13}$$

where the second term stabilizes the estimation and ε is a small value. We set ε to 10^{-2} in our experiment.

3.2.2 Probability Calculation

It is numerically difficult to compute the integration of Eq. (9) because the integration region $\hat{\boldsymbol{v}}_i + \mathcal{V}_\mathbf{0}$ is complex polytope in most lattices. Furthermore, with increasing dimensionality, the integral computations become impractical in terms of computational complexity. To resolve this, we introduce a Monte Carlo (MC) method (MacKay, 1998), which approximates integration as

$$\int_{\hat{\boldsymbol{v}}_i + \mathcal{V}_\mathbf{0}} \mathcal{N}(\boldsymbol{\mu}_i, \mathbf{C}_i)(\boldsymbol{x})\, d\boldsymbol{x} \approx \frac{1}{M} \sum_{j=1}^{M} \frac{\mathcal{N}(\boldsymbol{\mu}_i, \mathbf{C}_i)(\boldsymbol{x}_j)}{p(\boldsymbol{x}_j)}, \tag{14}$$

where $\boldsymbol{x}_j$ is an n-dimensional point sampled from arbitrary probability density function p. The method also has the advantage of being applicable to more complex probability distributions, since end-to-end optimization is possible as long as the probability density function and its derivative can be computed.

To further improve estimation accuracy, we adopt a Quasi-Monte Carlo (QMC) method (Radovic et al., 1996), which uses low-discrepancy sequences such as Halton, Sobol', and Faure sequences as sampling points. The advantage of the QMC method is a faster rate of convergence than the naive MC method. The QMC method has a rate of convergence close to $O(1/M)$, whereas the rate for the MC method is $O(1/\sqrt{M})$. Thus Eq. (14) is re-written as

$$\int_{\hat{\boldsymbol{v}}_i+\mathcal{V}_0} \mathcal{N}(\boldsymbol{\mu}_i, \mathbf{C}_i)(\boldsymbol{x})\, d\boldsymbol{x} \approx \frac{V}{M} \sum_{j=1}^{M} \mathcal{N}(\boldsymbol{\mu}_i, \mathbf{C}_i)(\boldsymbol{x}_j) \tag{15}$$

where $V = \frac{1}{p(\boldsymbol{x}_j)}$ represents the volume of the Voronoi region. In the experiment section, we employ Sobol's sequence as sampling points and set the number of sampling points, M, to 256 in training and 8192 in inference.

Since the MC/QMC method contains estimation error, the following two processes are introduced during inference to prevent decoding failure. First, when calculating the cumulative probabilities in both the encoder and the decoder, the cumulative probabilities are accumulated in order of the centroid closest to each estimated mean vector, as long as the cumulative value does not exceed 1. The feature vector is quantized to the nearest centroid with the smallest distance among calculated centroids. Second, the encoder and the decoder use the fixed samples, namely, they use the same (fixed) random seed when calculating the probability with the QMC method in order to match the probability values of the encoder and the decoder.

4 Experiments

We conducted simulations to verify the efficiency of the proposed method.

4.1 Network Architecture

Our network architecture is based on (Cheng et al., 2020) (See Appendix A.1 for details). N is channel size corresponding to the network capacity, which is set according to the bitrate as described below. As we use multivariate Gaussian model, the output of f_ψ requires $N(n+1)$ channels.

4.2 Experiment Conditions

We used Λ_{24} lattice ($n = 24$). The reason is that Λ_{24} gives the optimal representation for a uniform distribution. Hence it is expected that the proposed method brings its latent features towards a uniform distribution through a optimization process (A_2, D_4, E_8 in Sec. 4.3.1 are used for the same reason). We adopted a fast quantization method for LVQ, which does not need to store representative points and offers a low complexity as described in Appendix A.2. We used a subset of ImageNet dataset (Russakovsky et al., 2015), and randomly scaled and cropped them to the size of 192×192 during training. We used Adam optimizer(Kingma & Ba, 2015) with a batch size of 16. The learning rate was scheduled at 10^{-4} for the first 20 epochs, and reduced to 10^{-5} for the last 10 epochs. λ was set to $\{256, 1024, 2048, 4096\}$ and network channel size N was set to 144 for the lowest rate model and 192 for three higher rate models. For evaluation, we tested the Kodak image dataset (Kodak, 1993) consisting of 24 images (See Appendix B for other datasets). To evaluate the RD performance, the bitrate is measured by bits per pixel (bpp), and the quality is measured by PSNR, where bitrate and PSNR are calculated by averaging the encoding results for all 24 images. We plot the RD curves and calculate the Bjontegaard delta bitrate (BDBR) (Bjontegaard, 2001) to compare their coding efficiency. We compared the proposed method with VTM 15.0 (JVET), the reference software of the latest video coding standard H.266/VVC, with intra profile and H.265/HEVC-based encoder BPG (Bellard) and several of the learning-based methods. For VTM and BPG, the input RGB images were converted into YUV444 format and encoded, then the reconstructed images were converted into RGB and PSNR were calculated by averaging the MSE of each RGB value. For the

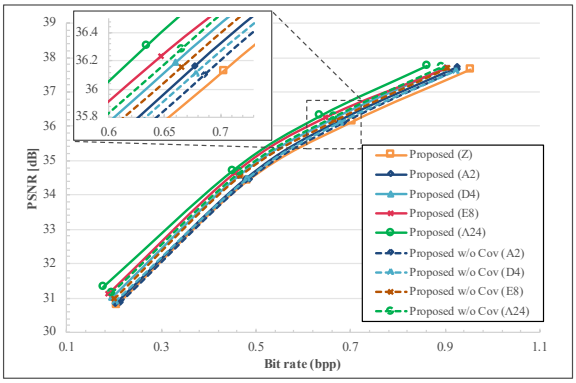

Figure 3: Comparison of RD performance for Kodak dataset for different number of dimensions and the use or non-use of a covariance matrix in the proposed method

Table 1: Comparison of BDBR for Kodak dataset for different numbers of dimensions and the use or non-use of a covariance matrix in the proposed method. $A_2, D_4, E_8, \Lambda_{24}$ are the optimal lattice quantizers for 2-, 4-, 8- and 24-dimension as mentioned Sec. 3.1.

Dimension n	**C**	**BDBR**
1 ($\mathbb{Z}$, scalar)	-	0.0 % (anchor)
2 (A_2)	-	0.0 %
	✓	-2.3 %
4 (D_4)	-	-1.8 %
	✓	-6.8 %
8 (E_8)	-	-6.3 %
	✓	-10.0 %
24 (Λ_{24})	-	-9.2 %
	✓	**-14.7 %**

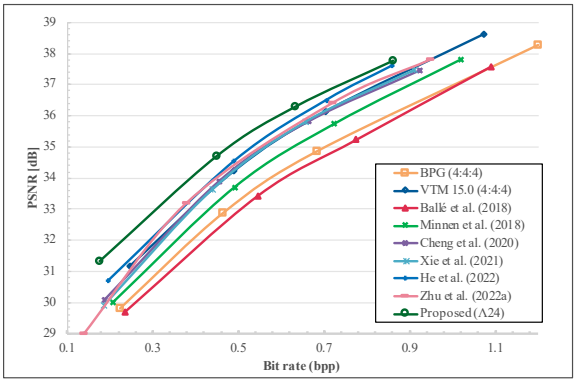

Figure 4: RD performance for Kodak dataset

Table 2: Comparison of BDBR for Kodak dataset

Method	**BDBR**
BPG (4:4:4)	23.8 %
VTM 15.0 (4:4:4)	0.0 % (anchor)
Ballé et al. (2018)	29.8 %
Minnen et al. (2018)	11.4 %
Cheng et al. (2020)	0.5 %
Xie et al. (2021)	1.4 %
He et al. (2022)	-6.4 %
Zhu et al. (2022a)	-2.7 %
Proposed (Λ_{24})	**-18.0 %**

learning-based methods, including the proposed method, we used RGB format as the input. For the proposed method, the bitrate is calculated by the estimated values ($-\log_2(p)$).

4.3 Results and Discussions

4.3.1 Ablation Study

In order to clarify the effect of the number of dimensions n of Lattice VQ and the use of the estimated covariance matrix in the proposed method, we additionally simulate in other dimensions ($n = 1$ ($\mathbb{Z}$, scalar quantization) , $n = 2(A_2)$, $n = 4(D_4)$, $n = 8(E_8)$) and compared the performance with and without the estimation of the covariance matrix. Without estimation of the covariance matrix, f_ψ output $2N$ channels (n means and n scales for each feature vector) and squared scales were aligned to the diagonal components of each matrix $\mathbf{C}_i$; the other elements were set to 0.

The results of RD curves and BDBR are shown in Fig. 3 and Tab. 1. As for the number of dimensions, it can be shown that RD performance increases with the number of dimensions. This is consistent with the property of VQ that the expected error decreases as the number of dimensions increases, and there is the potential for further increases in gain with dimensionality increases. Regarding the use of a covariance matrix, the results shows better performance when a covariance matrix is used. This suggests the presence of correlation within the feature vector, which could be eliminated by using a covariance matrix as mentioned Sec. 3.1.

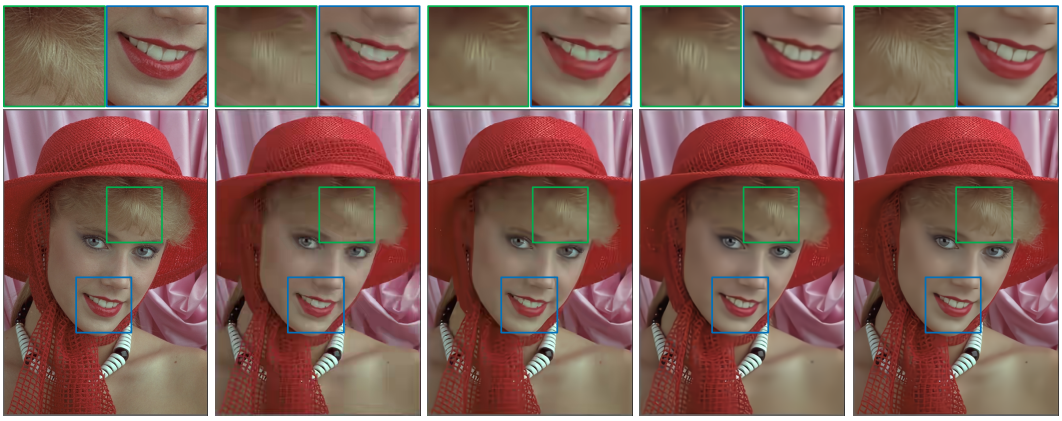

Figure 5: Reconstructed images of kodim04 (bpp, PSNR, MS-SSIM)

4.3.2 RD Performance

Fig. 4 and Tab. 2 show the results of comparison between the proposed method and existing methods in terms of RD performance. The results show that the proposed method gave better RD performance than all previous learning-based methods. Furthermore, the proposed method outperforms VTM 15.0 by 18.0 %.

4.3.3 Qualitative Evaluation

To evaluate the qualitative performance, we visualized the reconstructed images. Fig.5 shows reconstructed images at the level of approximately 0.1 bpp. In Fig. 5, the proposed method maintains more detail, such as the woman's hair and the contours of teeth, than the other methods. Moreover, it is observed that the other methods suffer from some artifacts and degradation.

5 Conclusion

This paper proposed a new VAE-based image compression method characterized by Lattice VQ for improving the hyperprior-based context-adaptive entropy model approach. The proposed method achieves end-to-end optimization with a hyperprior-based context-adaptive entropy model by approximating the likelihood calculation of latent feature vectors with high accuracy by using Monte Carlo integration. Furthermore, the proposed method provides highly accurate likelihood estimation by modeling the distribution parameters of latent feature vectors.

Experiments on public data sets showed that the proposed method achieves state-of-the-art RD performance compared to existing learning-based methods and outperforms VTM 15.0, the reference software of the latest video coding standard H.266/VVC, by 18.0 % for Kodak, 21.9 % for CLIC2022 and 39.2 % for Tecnick in the PSNR metric.

As a future work, we will address to reduce the complexity. This paper pursue maximizing coding efficiency rather than reducing complexity. Therefore, compared to the latest methods, the processing time due to the use of autoregressive models, etc. is large. In addition, in entropy coding, the amount of calculation of the cumulative probability table increases exponentially with the number of dimensions. These are prospective solutions in the following ways; the spatial autoregressive module, which is mainly dominant in network processing, could be solved by introducing the parallel computation mechanism such as (He et al., 2021) and entropy coding by restricting the number of representative points and introducing cascade estimation such as (Zhu et al., 2022a).

REFERENCES

E. Agrell, T. Eriksson, A. Vardy, and K. Zeger. Closest point search in lattices. *IEEE Transactions on Information Theory*, 48(8):2201–2214, 2002. doi: 10.1109/TIT.2002.800499.

Eirikur Agustsson, Fabian Mentzer, Michael Tschannen, Lukas Cavigelli, Radu Timofte, Luca Benini, and Luc Van Gool. Soft-to-hard vector quantization for end-to-end learning compressible representations. In Isabelle Guyon, Ulrike von Luxburg, Samy Bengio, Hanna M. Wallach, Rob Fergus, S. V. N. Vishwanathan, and Roman Garnett (eds.), *Advances in Neural Information Processing Systems 30: Annual Conference on Neural Information Processing Systems 2017, December 4-9, 2017, Long Beach, CA, USA*, pp. 1141–1151, 2017.

Eirikur Agustsson, Michael Tschannen, Fabian Mentzer, Radu Timofte, and Luc Van Gool. Generative adversarial networks for extreme learned image compression. In *2019 IEEE/CVF International Conference on Computer Vision, ICCV 2019, Seoul, Korea (South), October 27 - November 2, 2019*, pp. 221–231. IEEE, 2019. doi: 10.1109/ICCV.2019.00031.

Marc Antonini, Michel Barlaud, and Thierry Gaidon. Adaptive entropy-constrained lattice vector quantization for multiresolution image coding. In Petros Maragos (ed.), *Visual Communications and Image Processing '92*, volume 1818, pp. 441 – 457. International Society for Optics and Photonics, SPIE, 1992. doi: 10.1117/12.131462.

Nicola Asuni and Andrea Giachetti. TESTIMAGES: a large-scale archive for testing visual devices and basic image processing algorithms. In Andrea Giachetti (ed.), *Italian Chapter Conference 2014 - Smart Tools and Apps in computer Graphics, STAG 2014, Cagliari, Italy, September 22-23, 2014*, pp. 63–70. Eurographics, 2014. doi: 10.2312/stag.20141242. URL https://doi.org/10.2312/stag.20141242.

Johannes Ballé, Valero Laparra, and Eero P. Simoncelli. End-to-end optimized image compression. In *5th International Conference on Learning Representations, ICLR 2017, Toulon, France, April 24-26, 2017, Conference Track Proceedings*, 2017.

Johannes Ballé, David Minnen, Saurabh Singh, Sung Jin Hwang, and Nick Johnston. Variational image compression with a scale hyperprior. In *6th International Conference on Learning Representations, ICLR 2018, Vancouver, BC, Canada, April 30 - May 3, 2018, Conference Track Proceedings*, 2018.

F. Bellard. BPG image format. https://bellard.org/bpg/.

G. Bjontegaard. *Calculation of average PSNR differences between RD-curves*. VCEG-M33, 2001.

Benjamin Bross, Ye-Kui Wang, Yan Ye, Shan Liu, Jianle Chen, Gary J. Sullivan, and Jens-Rainer Ohm. Overview of the versatile video coding (VVC) standard and its applications. *IEEE Trans. Circuits Syst. Video Technol.*, 31(10):3736–3764, 2021. doi: 10.1109/TCSVT.2021.3101953.

Jianrui Cai and Lei Zhang. Deep image compression with iterative non-uniform quantization. In *2018 25th IEEE International Conference on Image Processing (ICIP)*, pp. 451–455, 2018. doi: 10.1109/ICIP.2018.8451411.

Jianrui Cai, Zisheng Cao, and Lei Zhang. Learning a single tucker decomposition network for lossy image compression with multiple bits-per-pixel rates, 2018.

Tong Chen, Haojie Liu, Zhan Ma, Qiu Shen, Xun Cao, and Yao Wang. End-to-end learnt image compression via non-local attention optimization and improved context modeling. *IEEE Transactions on Image Processing*, 30:3179–3191, 2021. doi: 10.1109/TIP.2021.3058615.

Zhengxue Cheng, Heming Sun, Masaru Takeuchi, and Jiro Katto. Learned image compression with discretized gaussian mixture likelihoods and attention modules. In *2020 IEEE/CVF Conference on Computer Vision and Pattern Recognition, CVPR 2020, Seattle, WA, USA, June 13-19, 2020*, pp. 7936–7945. Computer Vision Foundation / IEEE, 2020. doi: 10.1109/CVPR42600.2020.00796.

Karri Chiranjeevi and Uma Ranjan Jena. Image compression based on vector quantization using cuckoo search optimization technique. *Ain Shams Engineering Journal*, 9(4):1417–1431, 2018. ISSN 2090-4479. doi: https://doi.org/10.1016/j.asej.2016.09.009.

Yoojin Choi, Mostafa El-Khamy, and Jungwon Lee. Variable rate deep image compression with a conditional autoencoder. In *2019 IEEE/CVF International Conference on Computer Vision, ICCV 2019, Seoul, Korea (South), October 27 - November 2, 2019*, pp. 3146–3154. IEEE, 2019. doi: 10.1109/ICCV.2019.00324.

P.A. Chou, T. Lookabaugh, and R.M. Gray. Entropy-constrained vector quantization. *IEEE Transactions on Acoustics, Speech, and Signal Processing*, 37(1):31–42, 1989. doi: 10.1109/29.17498.

CLIC. Workshop and challenge on learned image compression. `http://compression.cc/`, 2022.

John Conway and N. Sloane. *Sphere Packings, Lattices and Groups*, volume 290. 01 1988. ISBN 978-1-4757-2018-1. doi: 10.1007/978-1-4757-2016-7.

John H. Conway and Neil J. A. Sloane. Fast quantizing and decoding and algorithms for lattice quantizers and codes. *IEEE Trans. Inf. Theory*, 28(2):227–231, 1982. doi: 10.1109/TIT.1982.1056484.

John H. Conway and Neil J. A. Sloane. Soft decoding techniques for codes and lattices, including the golay code and the leech lattice. *IEEE Trans. Inf. Theory*, 32(1):41–50, 1986. doi: 10.1109/TIT.1986.1057135.

Matthieu Courbariaux and Yoshua Bengio. Binarynet: Training deep neural networks with weights and activations constrained to +1 or -1. *CoRR*, abs/1602.02830, 2016.

Jeffrey De Fauw, Sander Dieleman, and Karen Simonyan. Hierarchical autoregressive image models with auxiliary decoders. *CoRR*, abs/1903.04933, 2019.

Google. WebP image format. `https://developers.google.com/speed/webp/`.

Vivek K. Goyal. Theoretical foundations of transform coding. *IEEE Signal Process. Mag.*, 18(5):9–21, 2001. doi: 10.1109/79.952802.

R. Gray. Vector quantization. *IEEE ASSP Magazine*, 1(2):4–29, 1984. doi: 10.1109/MASSP.1984.1162229.

Robert M. Gray and David L. Neuhoff. Quantization. *IEEE Trans. Inf. Theory*, 44(6):2325–2383, 1998. doi: 10.1109/18.720541.

Dailan He, Yaoyan Zheng, Baocheng Sun, Yan Wang, and Hongwei Qin. Checkerboard context model for efficient learned image compression. In *IEEE Conference on Computer Vision and Pattern Recognition, CVPR 2021, virtual, June 19-25, 2021*, pp. 14771–14780. Computer Vision Foundation / IEEE, 2021. doi: 10.1109/CVPR46437.2021.01453. URL `https://openaccess.thecvf.com/content/CVPR2021/html/He_Checkerboard_Context_Model_for_Efficient_Learned_Image_Compression_CVPR_2021_paper.html`.

Dailan He, Ziming Yang, Weikun Peng, Rui Ma, Hongwei Qin, and Yan Wang. ELIC: efficient learned image compression with unevenly grouped space-channel contextual adaptive coding. In *IEEE/CVF Conference on Computer Vision and Pattern Recognition, CVPR 2022, New Orleans, LA, USA, June 18-24, 2022*, pp. 5708–5717. IEEE, 2022. doi: 10.1109/CVPR52688.2022.00563. URL `https://doi.org/10.1109/CVPR52688.2022.00563`.

Yung-Han Ho, Chih-Chun Chan, Wen-Hsiao Peng, and Hsueh-Ming Hang. End-to-end learned image compression with augmented normalizing flows. In *IEEE Conference on Computer Vision and Pattern Recognition Workshops, CVPR Workshops 2021, virtual, June 19-25, 2021*, pp. 1931–1935. Computer Vision Foundation / IEEE, 2021. doi: 10.1109/CVPRW53098.2021.00220.

Yueyu Hu, Wenhan Yang, and Jiaying Liu. Coarse-to-fine hyper-prior modeling for learned image compression. In *The Thirty-Fourth AAAI Conference on Artificial Intelligence, AAAI 2020, The Thirty-Second Innovative Applications of Artificial Intelligence Conference, IAAI 2020, The Tenth AAAI Symposium on Educational Advances in Artificial Intelligence, EAAI 2020, New York, NY, USA, February 7-12, 2020*, pp. 11013–11020. AAAI Press, 2020.

ISO/IEC. ISO/IEC 14496-10 : Advanced Video Coding for Generic Audio-Visual Services, May 2003.

ISO/IEC. ISO/IEC 23008-2 : High Efficiency Video Coding, 2013.

ISO/IEC. ISO/IEC 23090-3 : Versatile Video Coding, 2020.

ISO/TEC. Information Technology — JPEG 2000 Image Coding System — Part 1: Core Coding System. ISO/IEC 15444-1:2004, October 2004.

ITU. ISO/IEC 10918-1 : 1993(E) CCIT Recommendation T.81. http://www.w3.org/Graphics/JPEG/itu-t81.pdf, 1993.

Nick Johnston, Damien Vincent, David Minnen, Michele Covell, Saurabh Singh, Troy Chinen, Sung Jin Hwang, Joel Shor, and George Toderici. Improved lossy image compression with priming and spatially adaptive bit rates for recurrent networks, 2017.

JVET. H.266/VVC Official Test Model VTM. `https://vcgit.hhi.fraunhofer.de/jvet/VVCSoftware_VTM/tree/VTM-15.0`.

Diederik P. Kingma and Jimmy Ba. Adam: A method for stochastic optimization. In *3rd International Conference on Learning Representations, ICLR 2015, San Diego, CA, USA, May 7-9, 2015, Conference Track Proceedings*, 2015.

Eastman Kodak. Kodak lossless true color image suite (photocd pcd0992). `http://r0k.us/graphics/kodak/`, 1993.

Shinobu Kudo, Shota Orihashi, Ryuichi Tanida, Seishi Takamura, and Hideaki Kimata. Gan-based image compression using mutual information for optimizing subjective image similarity. *IEICE Trans. Inf. Syst.*, 104-D(3):450–460, 2021.

Jooyoung Lee, Seunghyun Cho, and Seung-Kwon Beack. Context-adaptive entropy model for end-to-end optimized image compression. In *7th International Conference on Learning Representations, ICLR 2019, New Orleans, LA, USA, May 6-9, 2019*. OpenReview.net, 2019.

Jiaheng Liu, Guo Lu, Zhihao Hu, and Dong Xu. A unified end-to-end framework for efficient deep image compression, 2020.

David John Cameron MacKay. Introduction to monte carlo methods. In Michael I. Jordan (ed.), *Learning in Graphical Models*, volume 89 of *NATO ASI Series*, pp. 175–204. Springer Netherlands, 1998. doi: 10.1007/978-94-011-5014-9_7.

Detlev Marpe, Thomas Wiegand, and Gary J. Sullivan. The H.264/MPEG4 advanced video coding standard and its applications. *IEEE Commun. Mag.*, 44(8):134–143, 2006. doi: 10.1109/MCOM.2006.1678121.

Fabian Mentzer, Eirikur Agustsson, Michael Tschannen, Radu Timofte, and Luc Van Gool. Conditional probability models for deep image compression. In *2018 IEEE Conference on Computer Vision and Pattern Recognition, CVPR 2018, Salt Lake City, UT, USA, June 18-22, 2018*, pp. 4394–4402. Computer Vision Foundation / IEEE Computer Society, 2018. doi: 10.1109/CVPR.2018.00462. URL `http://openaccess.thecvf.com/content_cvpr_2018/html/Mentzer_Conditional_Probability_Models_CVPR_2018_paper.html`.

Fabian Mentzer, George Toderici, Michael Tschannen, and Eirikur Agustsson. High-fidelity generative image compression. In Hugo Larochelle, Marc'Aurelio Ranzato, Raia Hadsell, Maria-Florina Balcan, and Hsuan-Tien Lin (eds.), *Advances in Neural Information Processing Systems 33: Annual Conference on Neural Information Processing Systems 2020, NeurIPS 2020, December 6-12, 2020, virtual*, 2020.

David Minnen and Saurabh Singh. Channel-wise autoregressive entropy models for learned image compression. In *IEEE International Conference on Image Processing, ICIP 2020, Abu Dhabi, United Arab Emirates, October 25-28, 2020*, pp. 3339–3343. IEEE, 2020. doi: 10.1109/ICIP40778.2020.9190935. URL https://doi.org/10.1109/ICIP40778.2020.9190935.

David Minnen, Johannes Ballé, and George Toderici. Joint autoregressive and hierarchical priors for learned image compression. In Samy Bengio, Hanna M. Wallach, Hugo Larochelle, Kristen Grauman, Nicolò Cesa-Bianchi, and Roman Garnett (eds.), *Advances in Neural Information Processing Systems 31: Annual Conference on Neural Information Processing Systems 2018, NeurIPS 2018, December 3-8, 2018, Montréal, Canada*, pp. 10794–10803, 2018. URL https://proceedings.neurips.cc/paper/2018/hash/53edebc543333dfbf7c5933af792c9c4-Abstract.html.

Sayan Nag. Vector quantization using the improved differential evolution algorithm for image compression. *Genet. Program. Evolvable Mach.*, 20(2):187–212, 2019. doi: 10.1007/s10710-019-09342-8.

Igor Radovic, Ilya M. Sobol, and Robert F. Tichy. Quasi-monte carlo methods for numerical integration: Comparison of different low discrepancy sequences. *Monte Carlo Methods Appl.*, 2(1): 1–14, 1996. doi: 10.1515/mcma.1996.2.1.1.

Ali Razavi, Aäron van den Oord, and Oriol Vinyals. Generating diverse high-fidelity images with VQ-VAE-2. In Hanna M. Wallach, Hugo Larochelle, Alina Beygelzimer, Florence d'Alché-Buc, Emily B. Fox, and Roman Garnett (eds.), *Advances in Neural Information Processing Systems 32: Annual Conference on Neural Information Processing Systems 2019, NeurIPS 2019, December 8-14, 2019, Vancouver, BC, Canada*, pp. 14837–14847, 2019.

Oren Rippel and Lubomir D. Bourdev. Real-time adaptive image compression. In Doina Precup and Yee Whye Teh (eds.), *Proceedings of the 34th International Conference on Machine Learning, ICML 2017, Sydney, NSW, Australia, 6-11 August 2017*, volume 70 of *Proceedings of Machine Learning Research*, pp. 2922–2930. PMLR, 2017.

J. Rissanen and G. G. Langdon. Arithmetic coding. *IBM Journal of Research and Development*, 23 (2):149–162, 1979. doi: 10.1147/rd.232.0149.

Olga Russakovsky, Jia Deng, Hao Su, Jonathan Krause, Sanjeev Satheesh, Sean Ma, Zhiheng Huang, Andrej Karpathy, Aditya Khosla, Michael S. Bernstein, Alexander C. Berg, and Fei-Fei Li. Imagenet large scale visual recognition challenge. *Int. J. Comput. Vis.*, 115(3):211–252, 2015. doi: 10.1007/s11263-015-0816-y.

Mohd Fadzli Mohd Salleh and John J. Soraghan. A new multistage lattice vector quantization with adaptive subband thresholding for image compression. *EURASIP J. Adv. Signal Process.*, 2007, 2007. doi: 10.1155/2007/92928.

Shibani Santurkar, David M. Budden, and Nir Shavit. Generative compression. In *2018 Picture Coding Symposium, PCS 2018, San Francisco, CA, USA, June 24-27, 2018*, pp. 258–262. IEEE, 2018. doi: 10.1109/PCS.2018.8456298.

Y.H. Shin and C.-C. Lu. Image compression using vector quantization and artificial neural networks. In *Conference Proceedings 1991 IEEE International Conference on Systems, Man, and Cybernetics*, pp. 1487–1491 vol.3, 1991. doi: 10.1109/ICSMC.1991.169898.

Mikhail Shnaider and Andrew Peter Paplinski. *Still image compression with lattice quantization in wavelet domain*, pp. 56 – 119. Academic Press, United States of America, 1 edition, 2001. ISBN 0120147610.

Gary J. Sullivan, Jens-Rainer Ohm, Woojin Han, and Thomas Wiegand. Overview of the high efficiency video coding (HEVC) standard. *IEEE Trans. Circuits Syst. Video Technol.*, 22(12): 1649–1668, 2012. doi: 10.1109/TCSVT.2012.2221191.

Anna Tatsaki, Thanos Stouraitis, and Costas E. Goutis. Progressive image compression algorithm based on lattice vector quantization. In Naohisa Ohta, Heinz U. Lemke, and Jean Claude Lehureau (eds.), *Advanced Image and Video Communications and Storage Technologies*, volume 2451, pp. 228 – 236. International Society for Optics and Photonics, SPIE, 1995. doi: 10.1117/12.201201.

David S. Taubman and Michael W. Marcellin. *JPEG2000 - image compression fundamentals, standards and practice*, volume 642 of *The Kluwer international series in engineering and computer science*. Kluwer, 2002. ISBN 978-0-7923-7519-7. doi: 10.1007/978-1-4615-0799-4.

Lucas Theis, Wenzhe Shi, Andrew Cunningham, and Ferenc Huszár. Lossy image compression with compressive autoencoders. In *5th International Conference on Learning Representations, ICLR 2017, Toulon, France, April 24-26, 2017, Conference Track Proceedings*, 2017.

George Toderici, Sean M. O'Malley, Sung Jin Hwang, Damien Vincent, David Minnen, Shumeet Baluja, Michele Covell, and Rahul Sukthankar. Variable rate image compression with recurrent neural networks. In *4th International Conference on Learning Representations, ICLR 2016, San Juan, Puerto Rico, May 2-4, 2016, Conference Track Proceedings*, 2016.

George Toderici, Damien Vincent, Nick Johnston, Sung Jin Hwang, David Minnen, Joel Shor, and Michele Covell. Full resolution image compression with recurrent neural networks. In *2017 IEEE Conference on Computer Vision and Pattern Recognition, CVPR 2017, Honolulu, HI, USA, July 21-26, 2017*, pp. 5435–5443, 2017. doi: 10.1109/CVPR.2017.577.

Aäron van den Oord, Nal Kalchbrenner, Lasse Espeholt, Koray Kavukcuoglu, Oriol Vinyals, and Alex Graves. Conditional image generation with pixelcnn decoders. In Daniel D. Lee, Masashi Sugiyama, Ulrike von Luxburg, Isabelle Guyon, and Roman Garnett (eds.), *Advances in Neural Information Processing Systems 29: Annual Conference on Neural Information Processing Systems 2016, December 5-10, 2016, Barcelona, Spain*, pp. 4790–4798, 2016.

Aäron van den Oord, Oriol Vinyals, and Koray Kavukcuoglu. Neural discrete representation learning. In Isabelle Guyon, Ulrike von Luxburg, Samy Bengio, Hanna M. Wallach, Rob Fergus, S. V. N. Vishwanathan, and Roman Garnett (eds.), *Advances in Neural Information Processing Systems 30: Annual Conference on Neural Information Processing Systems 2017, December 4-9, 2017, Long Beach, CA, USA*, pp. 6306–6315, 2017.

Alexander Vardy and Yair Be'ery. Maximum likelihood decoding of the leech lattice. *IEEE Trans. Inf. Theory*, 39(4):1435–1444, 1993. doi: 10.1109/18.243466.

Teddy Voinson, Ludovic Guillemot, and Jean-Marie Moureaux. Image compression using lattice vector quantization with code book shape adapted thresholding. In *Proceedings of the 2002 International Conference on Image Processing, ICIP 2002, Rochester, New York, USA, September 22-25, 2002*, pp. 641–644. IEEE, 2002. doi: 10.1109/ICIP.2002.1040032.

Gregory K. Wallace. The JPEG still picture compression standard. *Commun. ACM*, 34(4):30–44, 1991. doi: 10.1145/103085.103089.

Will Williams, Sam Ringer, Tom Ash, David MacLeod, Jamie Dougherty, and John Hughes. Hierarchical quantized autoencoders. In Hugo Larochelle, Marc'Aurelio Ranzato, Raia Hadsell, Maria-Florina Balcan, and Hsuan-Tien Lin (eds.), *Advances in Neural Information Processing Systems 33: Annual Conference on Neural Information Processing Systems 2020, NeurIPS 2020, December 6-12, 2020, virtual*, 2020.

Yueqi Xie, Ka Leong Cheng, and Qifeng Chen. Enhanced invertible encoding for learned image compression. In Heng Tao Shen, Yueting Zhuang, John R. Smith, Yang Yang, Pablo Cesar, Florian Metze, and Balakrishnan Prabhakaran (eds.), *MM '21: ACM Multimedia Conference, Virtual Event, China, October 20 - 24, 2021*, pp. 162–170. ACM, 2021. doi: 10.1145/3474085.3475213.

Yifan Xue, Michael Q. Ding, and Xinghua Lu. Supervised vector quantized variational autoencoder for learning interpretable global representations. *CoRR*, abs/1909.11124, 2019.

Yibo Yang, Robert Bamler, and Stephan Mandt. Improving inference for neural image compression. In Hugo Larochelle, Marc'Aurelio Ranzato, Raia Hadsell, Maria-Florina Balcan, and Hsuan-Tien Lin (eds.), *Advances in Neural Information Processing Systems 33: Annual Conference on Neural Information Processing Systems 2020, NeurIPS 2020, December 6-12, 2020, virtual*, 2020.

Xiaosu Zhu, Jingkuan Song, Lianli Gao, Feng Zheng, and Heng Tao Shen. Unified multivariate gaussian mixture for efficient neural image compression. In *IEEE/CVF Conference on Computer Vision and Pattern Recognition, CVPR 2022, New Orleans, LA, USA, June 18-24, 2022*, pp. 17591–17600. IEEE, 2022a. doi: 10.1109/CVPR52688.2022.01709. URL https://doi.org/10.1109/CVPR52688.2022.01709.

Yinhao Zhu, Yang Yang, and Taco Cohen. Transformer-based transform coding. In *The Tenth International Conference on Learning Representations, ICLR 2022, Virtual Event, April 25-29, 2022*. OpenReview.net, 2022b. URL https://openreview.net/forum?id=IDwN6xjHnK8.

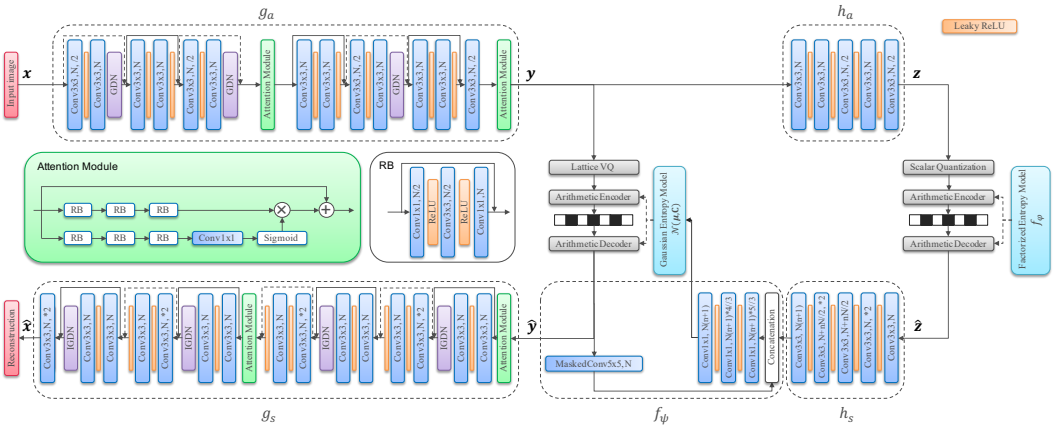

Figure 6: Network architecture

A Implementation Details

A.1 Network Architecture

Our network architecture is based on (Cheng et al., 2020) and is illustrated in Fig. 6. We use residual blocks and an attention module for both the feature encoder/decoder.

A.2 Low Complexity Lattice Vector Quantization

We used fast quantization method (Conway & Sloane, 1982) for A_2, D_4, E_8 and (Conway & Sloane, 1986) for Λ_{24}. These methods calculate the Euclidean norm for a several candidate points (ex. 256 points for Λ_{24}) for each vector and selects the one with the smallest norm among them. These methods have two advantages: one is that it does not need to keep representative points in memory, and the other is that the quantization process can be performed at high speed without calculating the distance to all quantized representative points as in the conventional VQ method.

B Additional Experiments

We also tested on the CLIC2022 test set (CLIC, 2022) consisting of 30 high resolution images, and Tecnick image dataset (Asuni & Giachetti, 2014) consisting of 40 images with 1200 x 1200 resolutions.

RD performance results for CLIC2022 are shown in Fig. 7 and Tab. 3 and for Tecnick are shown in Fig. 8 and Tab. 4

For both CLIC2022 and Tecnick, the proposed method also gave the state-of-the-art performance. Especially for Tecnick, it showed relatively large performance gains compared to Kodak and CLIC2022. This may be due to the fact that Tecnick has a lower texture component compared to Kodak and CLIC2022. The proposed method tends to produce higher gains at lower rates than at higher rates, which may have contributed to Tecnick's higher performance.

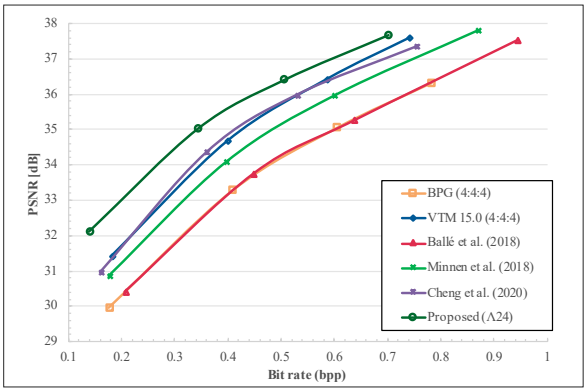

Figure 7: RD performance for CLIC2022 dataset

Table 3: Comparison of BDBR for CLIC2022 dataset

Method	BDBR
BPG (4:4:4)	40.9 %
VTM 15.0 (4:4:4)	0.0 % (anchor)
Ballé et al. (2018)	38.5 %
Minnen et al. (2018)	13.5 %
Cheng et al. (2020)	-0.8 %
Proposed (Λ_{24})	**-21.9 %**

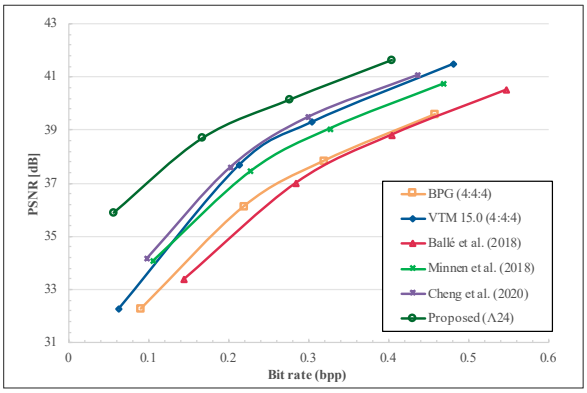

Figure 8: RD performance for Tecnick dataset

Table 4: Comparison of BDBR for Tecnick dataset

Method	BDBR
BPG (4:4:4)	45.8 %
VTM 15.0 (4:4:4)	0.0 % (anchor)
Ballé et al. (2018)	57.3 %
Minnen et al. (2018)	13.1 %
Cheng et al. (2020)	-1.5 %
Proposed (Λ_{24})	**-39.2 %**